Available online at www.sciencedirect.com

SCIENCE DIRECT®

Journal of Nuclear Materials 355 (2006) 83–88

journal of nuclear materials

www.elsevier.com/locate/jnucmat

High-dose neutron irradiation embrittlement of RAFM steels

E. Gaganidze *, H.-C. Schneider, B. Dafferner, J. Aktaa

Forschungszentrum Karlsruhe, Institut für Materialforschung II, P.O. Box 3640, 76021 Karlsruhe, Germany

Received 2 January 2006; accepted 21 April 2006

Abstract

Neutron irradiation-induced embrittlement of the reduced-activation ferritic/martensitic (RAFM) steel EUROFER97 was studied under different heat treatment conditions. Irradiation was performed in the Petten High Flux Reactor within the HFR Phase-IIb (SPICE) irradiation project up to 16.3 dpa and at different irradiation temperatures (250–450 °C). Several reference RAFM steels (F82H-mod, OPTIFER-Ia, GA3X and MANET-I) were also irradiated at selected temperatures. The impact properties were investigated by instrumented Charpy-V tests with subsize specimens. Embrittlement and hardening of as-delivered EUROFER97 steel are comparable to those of reference steels. Heat treatment of EUROFER97 at a higher austenitizing temperature substantially improves the embrittlement behaviour at low irradiation temperatures. Analysis of embrittlement in terms of the parameter $C = \Delta DBTT/\Delta\sigma$ indicates hardening-dominated embrittlement at irradiation temperatures below 350 °C with $0.17 \leqslant C \leqslant 0.53$ °C/MPa. Scattering of C at irradiation temperatures above 400 °C indicates no hardening embrittlement.

1. Introduction

Withstanding high neutron and heat flux is a crucial prerequisite for material qualification for future fusion reactors. Reduced-activation ferritic/martensitic (RAFM) steels are promising structure materials for first wall and blanket applications in future fusion power plants. Impact properties of modified commercial 10–11% Cr–NiMoVNb (MANET) steels as well as of newly developed RAFM 7–10% Cr–WVTa (OPTIFER, F82H) steels were studied thoroughly within the former irradiation programmes (FRUST/SIENA, MANITU, HFR-Ia, HFR-Ib) up to an irradiation damage dose of 2.4 dpa (MANET: 15 dpa) at different irradiation temperatures (250, 300, 350, 400 and 450 °C) [1–5]. Although newly developed RAFM steels exhibit a clearly better irradiation performance than modified commercial alloys, hardening induced by neutron irradiation, accompanied by embrittlement and reduced toughness and ductility, remain the main obstacle for their application, thus indicating further need for material improvement.

The present report focuses on the neutron irradiation-induced embrittlement and hardening of European reference steel for the first wall of a DEMO fusion reactor, 9%Cr–WVTa EURO-

* Corresponding author. Tel.: +49 7247 824083; fax: +49 7247 824566.
E-mail address: ermile.gaganidze@imf.fzk.de (E. Gaganidze).

0022-3115/$ - see front matter
doi:10.1016/j.jnucmat.2006.04.014

FER97. The steel was irradiated up to 16.3 dpa at different temperatures of 250, 300, 350, 400 and 450 °C. Irradiation performance of EUROFER97 is compared with the results obtained for the international reference steels F82H-mod, GA3X and OPTIFER-Ia.

2. Experimental

Embrittlement behaviour and hardening of materials have been quantified by impact testing. For a direct comparison with previously obtained results, the sub-sized Charpy-V specimens of KLST type (DIN 50115), see Fig. 1, were produced parallel to the rolling direction of the material plates (L–T orientation).

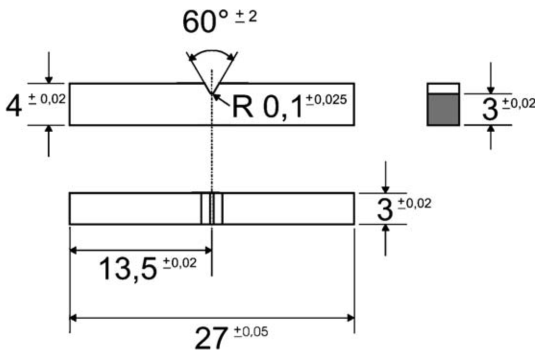

Fig. 1. Subsize Charpy specimen (all dimensions in mm).

An industrial batch of EUROFER97 steel was produced by Böhler Austria GmbH, see Table 1 for the steel's chemical composition. Part of the specimens (labelled EUROFER97 ANL) was machined from 25 mm thick EUROFER97 plates in the as-delivered state (i.e. austenitizing at 980 °C, followed by annealing at 760 °C). In order to study the influence of the higher austenitizing temperature on the laboratory scale, another part of the specimens (labelled EUROFER97 WB) was machined from EUROFER97 plates subjected to a heat treatment at a higher austenitizing temperature (at 1040 °C). For comparison, the heat treatment conditions of the reference alloys F82H-mod, GA3X, OPTIFER-Ia and martensitic steel MANET-I were identical to those of previous irradiation experiments [4,5]. Table 2 lists the heat treatment conditions along with selected properties of the investigated materials.

Table 1
Chemical composition of materials in wt% (n.s. stands for not specified)

Heat	EUROFER 97	Reference RAFM steels			10–11% Cr–NiMoVNb
		GA3X	F82H-mod	OPTIFER-Ia	MANET-I
	83697		9741	664	53645
Cr	8.91	9.17	7.7	9.33	10.8
W	1.08	2.12	2.04	0.965	n.s.
Mn	0.48	0.042	0.16	0.50	0.76
V	0.2	0.314	0.16	0.26	0.2
Ta	0.14	0.011	0.009	0.066	n.s.
C	0.12	0.159	0.09	0.10	0.14
Si	0.04	n.s.	0.11	0.06	0.37
P	0.005	n.s.	0.002	0.0046	0.005
S	0.004	n.s.	0.002	0.005	0.004
Ni	0.02	0.021	0.021	0.005	0.92
Mo	<0.001	0.0077	0.003	0.005	0.77
Nb	0.0017	0.011	0.0101	0.009	0.16
Al	0.009	0.015	0.0016	0.008	0.054
B	0.001	n.s.	0.0004	0.0062	0.0085
N	0.02	0.0018	0.008	0.0153	0.02
O	0.0008	n.s.	n.s.	n.s.	n.s.
Co	0.006	0.003	0.0037	n.s.	0.01
Cu	0.0015	0.0017	0.0063	0.035	0.015
Zr	<0.005	n.s.	0.01	n.s.	0.059
Ce	n.s.	n.s.	n.s.	<0.001	n.s.
Ti	0.006	0.001	0.004	0.007	n.s.
As	<0.005	n.s.	n.s.	0.0093	n.s.
Sb	<0.005	n.s.	n.s.	<0.0002	n.s.
Sn	<0.005	n.s.	n.s.	0.0005	n.s.
Fe	Balance	Balance	Balance	Balance	Balance

Table 2
Heat treatment and selected properties of unirradiated materials

Steel	Heat treatment	Grain size (μm)	USE (J)	DBTT (°C)	Dynamic yield stress (MPa)
EUROFER 97 ANL	980 °C/0.5 h + 760 °C/1.5 h	16 (14 mm plate)	9.84	−82	543 at 100 °C
EUROFER 97 WB	1040 °C/0.5 h + 760 °C/1.5 h	21.4 (14 mm plate)	9.84	−91	486 at 100 °C
GA3X	1000 °C/1 h + 700 °C/2 h	55 ± 5	9.4	−62	650 at 100 °C
F82H-mod	950 °C/0.5 h + 750 °C/2 h	55	9.7	−80	446 at 100 °C
OPTIFER-Ia	900 °C/0.5 h + 780 °C/2 h	10	10.6	−85	482 at 23 °C
MANET-I	980 °C/2 h + 1075 °C/0.5 h + 750 °C/2 h	30 ± 5	6.6	−30	670 at 100 °C

While OPTIFER alloys can be handled as medium-level waste after more than 100 years, F82H-mod and EUROFER97 may be considered low-level radioactive.

The specimens were irradiated within the framework of the HFR Phase-IIb SPICE (sample holder for irradiation of miniaturized steel specimens simultaneously at different temperatures) irradiation experiment in the Petten HFR [6]. The TRIO irradiation capsule equipped with the specially designed three sample holders was placed in one of the 9 in-core irradiation positions surrounded by fuel assemblies. After 771 full-power days, cumulative neutron fluences of 95.1×10^{24} and 127.0×10^{24} m^{-2} were achieved for thermal and fast ($E > 1.0$ MeV) neutrons at the centre-line specimen holder. The volume-averaged irradiation dose of 16.3 dpa in steel was determined on the basis of neutron metrology results. The nominal (actual) irradiation temperatures of 250 (244–260), 300 (285–301), 350 (339–354), 400 (382–400) and 450 °C (421–436 °C) were maintained by a proper balance between n,γ-heating and cooling with liquid sodium. Liquid sodium cooling provided for a highly improved temperature stability in comparison to the gas cooling used in former HFR experiments. EUROFER97 ANL specimens were irradiated at all irradiation temperatures. Due to the lack of irradiation space, the rest of the materials was irradiated at selected irradiation temperatures.

The instrumented impact tests on irradiated specimens were carried out with a newly built facility installed in the hot cells of the Fusion Materials Laboratory of the Institute. The facility is identical in construction with that used for the tests on unirradiated specimens. The test and evaluation procedures are identical with those employed in previous investigations [1–5]: 25 J pendulum impact hammer of a striker radius of 2 mm; distance between supports 22 mm; impact velocity 3.85 m/s; strain gauges applied in striker; PC-controlled test execution and recording, sampling rate 1 MHz; automatic specimen cooling, heating and transporting system; test temperature range between −180 and 600 °C.

The force vs. time curve was recorded for each experiment. For better analysis, these curves were subjected to a Fast Fourier Transformation (FFT) in order to filter out the oscillatory part of the system response. The deflection was calculated from the filtered force vs. time curves by solving the pendulum equation of motion taking into account its impact velocity. The impact energy (E) was then determined by integration of the force vs. deflection curves. The impact energies were plotted versus test temperature (T), see Fig. 2, and analysed with respect to the characteristic values of the Charpy upper shelf energy (USE, i.e. maximum in the energy versus temperature diagram) and the ductile-to-brittle transition temperature (DBTT). The latter was obtained by fitting the ductile-to-brittle transition region by a hyperbolic tangent function:

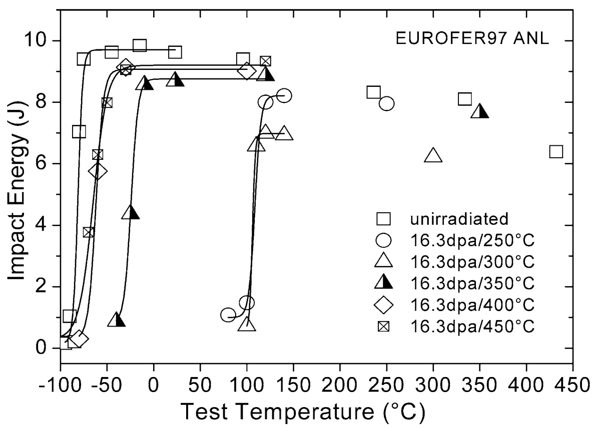

Fig. 2. Charpy impact energy vs. test temperature curves for unirradiated and 16.3 dpa (nominally) irradiated EUROFER97 ANL (irradiation conditions are given in the figure legend). The solid lines are fits according to Eq. (1).

$$E = \frac{\mathrm{LSE} + \mathrm{USE}}{2} + \frac{\mathrm{USE} - \mathrm{LSE}}{2} \times \tanh\left(\frac{T - \mathrm{DBTT}}{r}\right) \quad (1)$$

with LSE being the impact energy in the lower shelf and r the fitting parameter related to the slope of the curve in the ductile-to-brittle transition region.

About 5 or 6 specimens for each material and each irradiation temperature ensured a sufficient number of measurement points for plotting the Charpy energy vs. test temperature curves. Fig. 2 shows exemplarily the impact properties of unirradiated and irradiated EUROFER97 ANL along with the curve fits by Eq. (1).

The dynamic yield stress (σ_{Dy}) was derived from the filtered force vs. deflection curves at the onset of plastic deformation as stated in [2]:

$$\sigma_{\mathrm{Dy}} = \frac{C_g M_{\mathrm{bgy}}}{B(W - a_0)^2}, \quad (2)$$

where C_g is a constraint factor (2.99 for V-notch), M_{bgy} the bending moment at the point of general yield, B the specimen thickness (3 mm), W the specimen width (4 mm), and a_0 the notch depth (1 mm). The bending moment is related to the yield force F_{gy} by $M_{\mathrm{bgy}} = F_{\mathrm{gy}}L/4$, with L being the distance between the supports (22 mm).

Table 2 summarizes the dynamic yield stress at 100 °C for the unirradiated materials investigated.

3. Results and discussion

The results obtained by analysing the Charpy energy vs. test temperature curves are presented in Figs. 3–5.

Fig. 3 shows the USE as a function of irradiation temperature (T_{irr}). At low irradiation temperatures ($T_{\mathrm{irr}} \leqslant 300$ °C), the USE of EUROFER97 ANL is strongly affected by neutron irradiation, this effect being most pronounced at 300 °C. The USE recovers at higher irradiation temperatures ($T_{\mathrm{irr}} \geqslant 350$ °C), though it still remains below the USE under unirradiated conditions of 9.8 J. The impact toughness properties of EUROFER97 WB are influenced by 250, 350 and 450 °C neutron irradiation in quite similar ways. The reference steel OPTIFER-Ia irradiated at 300 °C shows the highest USE of 8.1 J, while the USE of F82H-mod irradiated at the same temperature is comparable to that of EUROFER97 ANL. MANET-I shows the worst impact toughness

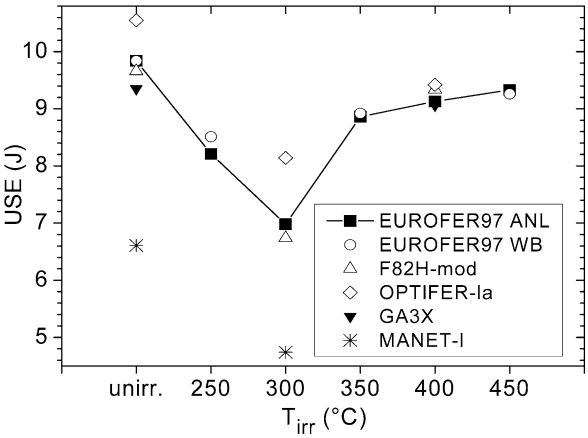

Fig. 3. Upper shelf energy vs. irradiation temperature (materials are indicated in the figure legend). For comparison, the results obtained under unirradiated conditions are included.

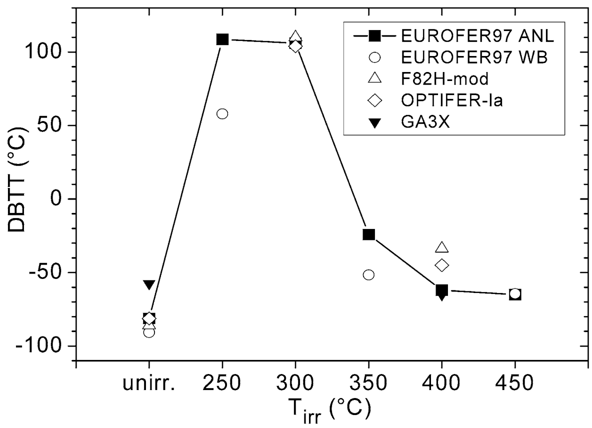

Fig. 4. Ductile-to-brittle transition temperature vs. irradiation temperature (materials are indicated in the figure legend). For comparison, the results obtained under unirradiated conditions are also included.

after neutron irradiation at 300 °C. Remarkably, the impact properties of MANET-I validated the previous results obtained within the framework of the FRUST/SIENA irradiation experiment performed in 1987–1990 [1]. The results of OPTIFER-Ia, F82H-mod and GA3X irradiated at 400 °C show USE comparable to that of EUROFER97 ANL. As inferred from Table 2, the grain size cannot simply be correlated with the upper shelf energy. However, the finest grain structure of OPTIFER-Ia might explain the superior USE of OPTIFER-Ia under unirradiated and irradiated conditions.

Fig. 4 shows the DBTT as a function of irradiation temperature. The DBTT of all materials investigated is influenced most at low irradiation temperatures

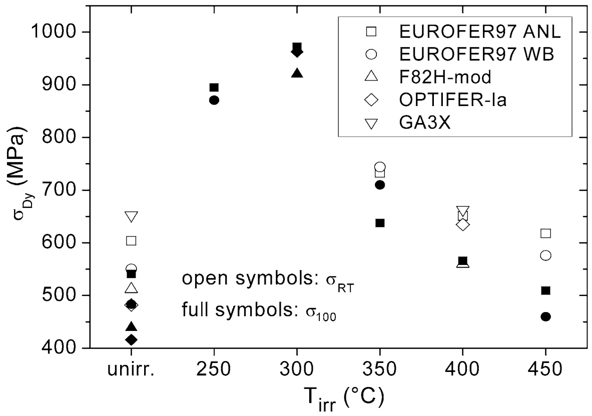

Fig. 5. Dynamic yield stress vs. irradiation temperature (materials are indicated in the figure legend); open symbols: σ_{RT}, full symbols σ_{100}, see text for explanation. For comparison, the results obtained under unirradiated conditions are presented as well.

($T_{irr} \leqslant 300$ °C). Remarkably, the DBTT of EUROFER97 WB at $T_{irr} = 250$ °C is smaller than the DBTT of EUROFER97 ANL by 50 °C. The difference of the DBTTs of EUROFER97 materials austenitized at different temperatures decreases with increasing irradiation temperature and vanishes completely at 450 °C. The DBTT of reference F82H-mod and OPTIFER-Ia materials is comparable to that of EUROFER97 ANL at $T_{irr} = 300$ °C. However, it has to be mentioned that for F82H-mod, the slope (r parameter) of the curve in the transition region is smaller (larger) than the corresponding slopes (r parameters) of EUROFER97 ANL and OPTIFER-Ia specimens. The DBTTs of the materials irradiated above 400 °C remain below −30 °C and, hence, are well below the material application temperature. The GA3X steel shows a negative shift in DBTT at 400 °C irradiation temperature – a behaviour already observed under 0.8 dpa/450 °C irradiation condition [4]. For boron contents below 62 wppm, the influence of boron-to-helium transformation on embrittlement cannot be resolved for 16.3 dpa-irradiated steels, in clear contrast to higher boron contents and lower irradiation doses (up to 2.4 dpa), where ^{10}B burn-up indeed contributes to embrittlement to a large extent [3,5].

The hardening behaviour of the irradiated materials is shown in Fig. 5, where the dynamic yield stress is plotted as a function of the irradiation temperature. The unirradiated values of the σ_{Dy} are also included for comparison, see Table 2. Two test temperature bins have been defined for yield stress analysis: (a) RT and (b) 100–120 °C (nominal 100 °C). EUROFER97 ANL shows strong hardening ($\Delta\sigma_{Dy}$) at low irradiation temperatures that is most pronounced for irradiation at 16.3 dpa/300 °C. The hardening of EUROFER97 ANL is substantially reduced at higher irradiation temperatures ($T_{irr} \geqslant 350$ °C), which is in clear agreement with our previous observation at lower irradiation doses up to 2.4 dpa [4,5].

The hardening vs. embrittlement behaviour was quantified in terms of the hardening shift coefficient C defined as $C = \Delta\text{DBTT}/\Delta\sigma$ [7,8]. Fig. 6 displays this parameter for two test temperature bins at room temperature (C_{RT}) and at 100–120 °C (C_{100}). At $T_{irr} \leqslant 350$ °C, the coefficient C_{100} varies between $0.17 \leqslant C_{100} \leqslant 0.53$ °C/MPa, which is in good agreement with the analysis of 7–9% Cr RAFM steels yielding $C = (0.38 \pm 0.18)$ °C/MPa [7] and indicating that embrittlement is dominated by a hardening mechanism. The hardening shift coefficient C_{100} tends to increase at $T_{irr} = 400$ °C. This suggests a non-hardening embrittlement (NHE) mechanism that primarily occurs under thermal aging conditions. Depending on the nature of the dominating NHE mechanism, the coefficient C may become large, very small or even negative at $T_{irr} \geqslant 400$ °C in case of material softening [7,8]. Indeed, such a behaviour was observed for EUROFER97 ANL, EUROFER97 WB and GA3X as shown in Fig. 6.

The shift in DBTT vs. irradiation dose is plotted in Fig. 7 for EUROFER97 steel irradiated between 300 and 330 °C. For comparison, the data reported in [9] and [10] are presented as well. Large data scattering at low and intermediate doses prevents

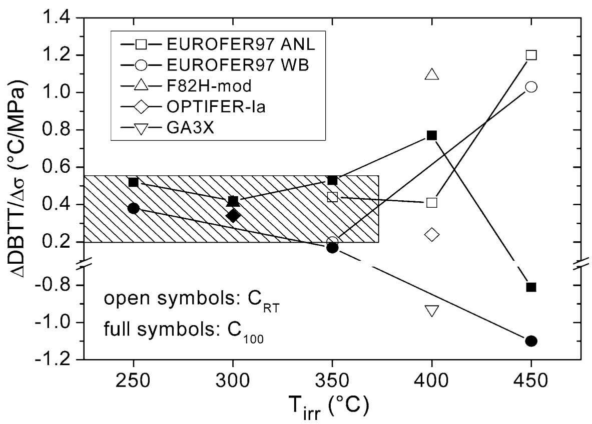

Fig. 6. Hardening shift coefficient C vs. irradiation temperature (materials are indicated in the figure legend); open symbols: C_{RT}, full symbols C_{100}, see text for explanation. The dashed area indicates the scattering band for C from [7,8].

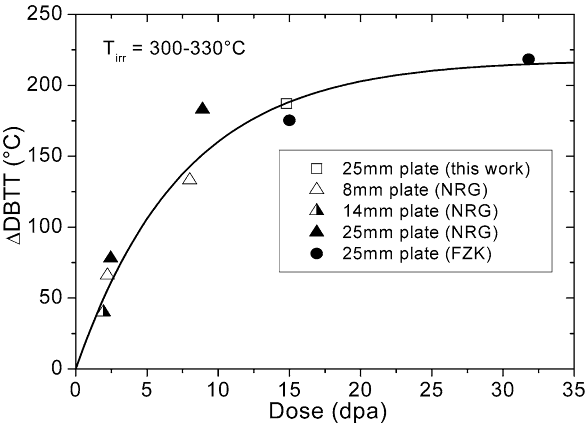

Fig. 7. Shift in DBTT vs. irradiation dose for EUROFER97. The triangles ($T_{irr} = 300$ °C) are from [9] and circles ($T_{irr} = 330$ °C) from [10]. The line is the $\Delta DBTT = \Delta DBTT_{sat}(1 - \exp(-Dose/Dose_0))$ fit for the presented data, with $\Delta DBTT_{sat}$ and $Dose_0$ as fitting parameters. The weighted least square method by minimizing the sum $\Sigma[(\Delta DBTT_{fit} - \Delta DBTT)^2/\Delta DBTT^2]$ resulted in $\Delta DBTT_{sat} = 218.1$ °C and $Dose_0 = 7.54$ dpa.

a quantitative analysis of the embrittlement trend. Furthermore, it has to be noted that the dose of 32 dpa was achieved at 330 °C [10]. As shown here, the shift in DBTT is very sensitive to the irradiation temperature between 300 and 350 °C and substantially decreases at 350 °C. Having all these facts in mind, no unambiguous estimation of embrittlement saturation is possible on the basis of the data available. Consequently, embrittlement data at higher irradiation doses are indispensable for a structure material qualification.

4. Conclusion

The European RAFM reference steel EUROFER97 irradiated up to 16.3 dpa at 250, 300, 350, 400 and 450 °C showed an embrittlement behaviour and hardening comparable to that of the best reference RAFM steels. At $T_{irr} = 300$ °C, the DBTT and dynamic yield stress of EUROFER97 are comparable to those of OPTIFER-Ia. The latter showed the best impact toughness at $T_{irr} = 300$ °C. The embrittlement behaviour of the reference material F82H-mod at $T_{irr} = 300$ °C is somewhat worse than that of EUROFER97 ANL. It is characterised by a large impact energy scattering in the ductile-to-brittle transition region. At $T_{irr} = 400$ °C, the embrittlement behaviour of EUROFER97 is superior to that of OPTIFER-Ia and F82H-mod, though the DBTTs of these materials remain below −30 °C. Heat treatment of the as-delivered EUROFER97 plate led to the reduction of embrittlement at low irradiation temperatures. The hardening shift coefficient C varied between $0.17 \leqslant C_{100} \leqslant 0.53$ °C/MPa at $T_{irr} \leqslant 350$ °C, which is in good agreement with literature [7,8] and indicates a hardening embrittlement mechanism. The state-of-the-art structure materials are highly suited for the special fusion reactor design with the operating temperature range for the first wall and blanket modules being between 350 and 450 °C.

Acknowledgements

The authors would like to thank to R. Rolli, head of the hot cells of the Fusion Materials Laboratory, and his staff member H. Ries for the execution of the Charpy impact tests on irradiated specimens. This work, supported by the European Communities under the contract of Association between EURATOM and Forschungszentrum Karlsruhe, was carried out within the framework of the European Fusion Development Agreement. The views and opinions expressed herein do not necessarily reflect those of the European Commission.

References

[1] M. Rieth, B. Dafferner, C. Wassilew, Der Einfluss von Wärmebehandlung und Neutronenbestrahlung auf die Kerbschlageigenschaften des martensitischen 10,6% Cr–Stahls MANET-I, Institut für Materialforschung, Kernforschungszentrum Karlsruhe, KfK-Bericht 5243, September (1993).

[2] M. Rieth, B. Dafferner, H.-D. Röhrig, J. Nucl. Mater. 233–237 (1996) 351.

[3] M. Rieth, B. Dafferner, H.-D. Röhrig, J. Nucl. Mater. 258–263 (1998) 1147.

[4] H.-C. Schneider, B. Dafferner, J. Aktaa, J. Nucl. Mater. 295 (2001) 16.

[5] H.-C. Schneider, B. Dafferner, J. Aktaa, J. Nucl. Mater. 321 (2003) 135.

[6] J. Ahlf, A. Zurita, High Flux Reactor (HFR) Petten – Characteristics of the Installation and the Irradiation Facilities, Nuclear Science and Technology, Report EUR 15151 EN (1993).

[7] T. Yamamoto, H. Kishimoto, G.R. Odette, Fusion Materials Semiannual Report 7/1 to 12/31/2003 DOE/ER-313/34.

[8] G.R. Odette, T. Yamamoto, H.J. Rathbun, M.Y. He, M.L. Hribernik, J.W. Rensman, J. Nucl. Mater. 323 (2003) 313.

[9] J. Rensman, E. Lucon, J. Boskeljon, J. van Hoepen, R. den Boef, P. ten Pierick, J. Nucl. Mater. 329–333 (2004) 1113.

[10] C. Petersen, A. Povstyanko, V. Prokhorov, A. Fedoseev, O. Makarov, B. Dafferner, Proceedings of ICFRM-12, December 4–10, 2005, Santa-Barbara, USA (in press).